RSC Advances

PAPER

View Article Online
View Journal | View Issue

Cite this: *RSC Adv.*, 2024, **14**, 2027

Injectable, thermo-sensitive and self-adhesive supramolecular hydrogels built from binary herbal small molecules towards reusable antibacterial coatings†

Zhibin Dong,[a] Fengjun Ma,[a] Xiaocen Wei,[a] Linlin Zhang,[a] Yongling Ding,[b] Lei Shi, *[a] Chen Chen, [a] Yuxia Ma*[a] and Yuning Ma *[a]

Received 17th November 2023
Accepted 4th January 2024

DOI: 10.1039/d3ra07882e

rsc.li/rsc-advances

Herbal hydrogels as a new class of sustainable functional materials have attracted extensive attention. However, the development of herbal hydrogels is significantly hindered due to their poor hydrogel performances and the lack of universal preparation methods. In this study, four herbal hydrogels composed of phytochemical polyphenols and stevioside compounds are prepared through a facile heating-cooling process, where multiple hydrogen bonding interactions between two monomers provide the main driving force for gelation. These herbal hydrogels exhibit thermo-sensitivity and good reversibility (25–90 °C), robust adhesion behaviours on hydrophilic and hydrophobic surfaces (maximum adhesion strength of 591.7 kPa), and outstanding antibacterial properties (100% bacteriostatic ratio). Profiting from these intriguing characteristics, they are demonstrated to show great potential as natural antibacterial coatings by depositing thin hydrogel layers onto diverse substrates. More importantly, the hydrogel coatings could be easily recycled by thermal regelation and reused at least 5 times. This work proposes a simple and universal strategy for preparing functional hydrogels based on binary herbal small molecules, which also sheds light on the development of reusable hydrogel coatings.

1. Introduction

Developing functional hydrogel materials based on naturally occurring small molecules, especially renewable resources, has attracted great interest in recent years owing to their fascinating advantages in availability and biocompatibility and promising applications in drug delivery, tissue engineering, and antibacterial materials.[1–4] Herbal small molecules as a new kind of natural building block bearing intrinsically abundant structural diversity have been reported to directly self-assemble into hydrogels.[5–8] As an emerging field, the current research on such herbal hydrogels focuses on their biological activities after self-assembly.[9] For instance, rhein molecules could self-assemble into a stable hydrogel through noncovalent interactions and possess better therapeutic efficacy (*e.g.*, long-lasting effect and decreased cytotoxicity) in comparison to that of free drugs.[10] Yet, to date the performances of herbal hydrogels are still poor in terms of mechanical property, adhesion strength and processability. Thus, it is highly desirable to exploit herbal hydrogels with enhanced properties and facilitate their applications in different health-related fields.

Nowadays, the herbal hydrogels are mainly built from single-component herbal small molecules benefiting from their unique self-assembly abilities. Glycosides,[11,12] flavonoids,[13,14] steroids,[15] and others[16,17] with different skeletons have been found to be natural gelators, whose self-assembly are driven by noncovalent interactions including electrostatic interaction, hydrophobic interaction, hydrogen bonding, π–π interaction, and van der Waals forces.[18] Though great progress has been made, no universal and effective strategies have been validated for obtaining herbal hydrogels. On one hand, the screen process from large amounts of herbal small molecules is serendipitous and time-consuming. On the other hand, complex but matched intermolecular interactions required in the assembly system remarkably restrict the selection of suitable herbal monomers. In fact, the available herbal hydrogels are limited, severely hindering the studies of structure–property relationship and further exploration of new preparation approaches. Therefore, simple and universal strategies for preparing herbal hydrogels are urgently needed.

Hydrogen bonding is a kind of intermolecular forces that exists in nature[19] and has been widely adopted for developing

[a]*Department of Acupuncture-Moxibustion and Tuina, Key Laboratory of New Material Research Institute, Institute of Pharmacy, Shandong University of Traditional Chinese Medicine, Jinan 250355, P.R. China. E-mail: 60230082@sdutcm.edu.cn; myxia1976@163.com; myning0405@163.com*

[b]*School of Transportation Civil Engineering, Shandong Jiaotong University, Jinan, 250357, P.R. China*

† Electronic supplementary information (ESI) available. See DOI: https://doi.org/10.1039/d3ra07882e

functional materials such as deep eutectic solvents,[20,21] elastomers,[22,23] and hydrogels,[24–26] and so on. Moreover, intriguing properties of high-strength, stimuli-responsiveness, self-healing, and strong adhesion could be obtained in these materials due to robust and adaptable hydrogen bonding networks. Herbal small molecules like polyphenols and stevioside compounds are characterized by abundant hydroxyl and carboxyl groups within their structures, which endow them with powerful abilities to form hydrogen bonding.[27,28] It is envisioned that using the two kinds of herbal monomers as building blocks may enable the formation of three-dimensional (3D) hydrogen bonding networks, thus achieving new binary herbal hydrogels with advanced functions.

Herein, in this work, phytochemical-based polyphenols (*e.g.*, epigallocatechin gallate (EGCG), procyanidin (PC), tannic acid (TA) and tea polyphenols (TP)) and two stevioside compounds of stevioside (St) and rebaudioside A (RA) were employed to explore the preparation of binary herbal hydrogels. Based on this, four herbal hydrogel systems were verified, where the polyphenols served as hydrogen bond donors while the steviosides played the role of hydrogen bond acceptors. It was found that these herbal hydrogels possessed injectability, thermo-responsiveness, strong adhesion on both hydrophilic and hydrophobic surfaces, and excellent antibacterial property. Thanks to these appealing features, they were deposited onto various substrates as hydrogel coatings *via* a facile coating method. Besides, the hydrogel coatings could be reused through recycling–remolding process. The present study provides a universal method for the preparation of functional hydrogels based on binary herbal small molecules, which hold great potential as sustainable antibacterial coatings.

2. Materials and methods

2.1 Materials

Epigallocatechin gallate was purchased from Meryer. Procyanidin, tannic acid, and stevioside were obtained from Aladdin. Tea polyphenols and rebaudioside A were the products of Shanghai Yuanye Bio-Technology Co., Ltd. The chemicals were used as purchased without further purification, and the ultrapure water (18.2 MΩ) was used throughout the experiments.

2.2 Fabrication of herbal hydrogels

Taking EGCG–St hydrogel as an example, EGCG (1.83 g, 2.0 M) and St (4.02 g, 2.5 M) were placed in a glass bottle, and 2 mL water was added. Then, the glass bottle was sealed and continuously heated at 80 °C in a laboratory oven for about 18 h. Until the two monomers were completely dissolved, the mixture system was left at room temperature to trigger the formation of hydrogels. Similar procedure was adopted for the preparation of other herbal hydrogels except that the monomers and their corresponding amounts were different (Table S1†).

2.3 Characterization

2.3.1 General measurements. FT-IR spectra were acquired using the FT-IR spectrometer (Frontier, PerkinElmer, USA) and the scanning range was 4000–400 cm^{-1} with a spectral resolution of 4 cm^{-1}. ^1H NMR and 2D ROESY NMR characterizations were performed with an ADVANCE III HD-600 MHz spectrometer (Bruker, USA) using D_2O as the solvent. Powder X-ray diffraction spectra were collected on a Burker D8 Discover with Cu-Kα (1.5405 Å) radiation at room temperature with a 2θ range of 5–90°. The SEM investigations of lyophilized herbal hydrogels were conducted on a scanning electron microscope (TESCAN MIRA LMS, Czech Republic) operated at an acceleration voltage of 3 kV.

2.3.2 Rheological tests. The rheological studies were carried out on a rotational rheometer (AR-G2, TA Instruments, USA). The strain-dependent oscillation was measured at 0.01% to 10% with a frequency of 10 Hz. The dynamic frequency sweep was measured at 0.1% strain and the frequency was between 0.1 and 100 Hz. The dynamic time sweep was measured at 0.1% strain and the time was kept at 600 s. The temperature-dependent rheology measurement was performed at 0.1% strain and 10 rad s^{-1} angular frequency. Viscosity measurement data were obtained from steady-state testing in a shear rate range of 0.01–100 s^{-1}. The exposed surfaces of the samples were covered with a thin layer of glycerol preventing evaporation of water during all the tests.

2.3.3 Adhesion tests. The adhesion tests were conducted on an electronic universal testing machine (XWN-20, Institute of Experimental Instrument, China) using the lap-shear testing method. Briefly, the hydrogel sample was placed between two pieces of substrates including wood, steel, ceramics, glass, plastics, and PTFE and the substrates were stretched to separation at a speed of 10 mm min^{-1}. The adhesion strength was calculated by the measured maximum tensile force (N) divided by the adhesion area (m^2) of the hydrogel on substrates.

2.4 *In vitro* antibacterial assays

The antibacterial properties of herbal hydrogels were evaluated by the flat colony counting method. *E. coli* (ATCC 25922) and *S. aureus* (ATCC 29213) were chosen as Gram-negative and Gram-positive bacteria, respectively. The detailed procedure was as follows: first, the hydrogel sample was placed in a 24 well plate and exposed under a UV lamp for 30 min; then 30 μL of the 1.0 $\times 10^6$ CFU mL^{-1} bacterial stock solution in liquid Luria–Bertani medium was introduced to the surface of the given hydrogel and incubated at 37 °C for 18 h. 870 μL sterile PBS solution was added to each well and bacteria on hydrogel surface were ultrasonically detached. After serial 10-fold dilutions of the previous bacterial solution, the bacterial suspension (100 μL) was spread evenly on a solid Luria–Bertani medium and incubated at 37 °C for 24 h. Last, the number of bacterial colonies was recorded and counted by digital camera. The *in vitro* bactericidal activity was determined by counting the bacterial colonies. For comparison, identical bacterial suspensions without the addition of hydrogel were used as the control group.

2.5 Fabrication of antibacterial coatings

The preparation of antibacterial coatings was carried out on a coating machine (CHTB-07, START, China). Before the coating

process, the substrates were cleaned and sterilized under a UV lamp for 30 min. The hydrogel sample was directly casted on the surfaces of different substrates, and the thickness of antibacterial coatings was controlled to be 0.3 mm with a coating speed of 8 mm s^{-1}.

3. Results and discussion

3.1 Construction of herbal hydrogels

In this study, the co-assembly herbal hydrogels were formed by heating the mixture of polyphenols and stevioside compounds to fully dissolve and subsequently cooling to room temperature. The detailed preparation conditions were listed in Table S1.† Taking EGCG–St hydrogel as an example, the irreversible transition of EGCG and St molecules from solid mixture to a homogeneous and viscous solution after heating at 80 °C was clearly observed, and then the cooling process triggered the formation of hydrogels (Fig. 1a). The water content was calculated to be 25.5 wt% for EGCG–St hydrogel. As shown in Fig. S1,† three other hydrogels were also obtained in a same way regardless of the macroscopic states of pure herbal small molecules. The easy extension of hydrogel precursors to different natural polyphenols and stevioside compounds possessing similar chemical and structural features revealed a good universality of this preparation method. In addition, the gelation time was about 10 min for different hydrogel systems, suggesting rapid gelation kinetics. The appearance of obtained EGCG–St hydrogel was orange-red, which could be molded into various shapes including circular-, quadrate-, and heart-shaped ones (Fig. 1b). Then powder X-ray diffraction (XRD) measurements were carried out to figure out its inner structural characteristics (Fig. 1c). It can be found that no characteristic peaks attributable to St monomers occurred while EGCG exhibited a series of distinct diffraction peaks consistent with its crystalline nature.[29] On the contrary, the XRD results confirmed the amorphous nature of EGCG–St hydrogel, suggesting that co-assembly behaviour hindered the crystallization of monomers. Moreover, scanning electron microscopy (SEM) revealed a nonporous microstructure of EGCG–St hydrogel. Similar XRD and SEM characterization results were observed for other hydrogels (Fig. S2 and S3†). Thus, a conclusion could be drawn that disordered and dense 3D hydrogel network was dominant in the binary herbal hydrogels based on the above results.

3.2 Assembly mechanism of herbal hydrogels

As shown in Fig. 2a, pure EGCG (2.0 M) and St (2.5 M) in water only formed solution or viscous sol while mixing them yielded stable and uniform EGCG–St hydrogel. This significant difference indicated the existence of intermolecular interactions between EGCG and St monomers and their crucial role in promoting gelation. Fig. 2b depicts chemical structures of the polyphenols and stevioside, and it is worth noting that neither positive nor negative charges were accommodated in their structural backbones. Meanwhile, the stevioside compounds have no cyclic π-electron systems. Given these structural features, electrostatic interactions and π–π stacking should be unlikely to emerge in the present hydrogels, but there is a great possibility for polyphenols and stevioside compounds to form multiple hydrogen bonding interactions.

The formation of hydrogen bonding and relevant co-assemble mode were decrypted first using Fourier transform infrared spectroscopy, and the results of EGCG, St, and EGCG–St hydrogel are shown in Fig. 3a and S4.† After the formation of hydrogels, EGCG's –CH aromatic in-plane bending centered at 958 and 854 cm^{-1} disappeared. Compared with the asymmetric and symmetric stretching vibrations of sp^3-CH in St at 2926 and 2876 cm^{-1}, those of the EGCG–St hydrogel were around 2936 and 2884 cm^{-1} with an obvious increase. These changes pointed to that the aromatic rings of EGCG and glucose rings in St were the interaction sites in hydrogels. ^{1}H NMR of EGCG and St mixture was tested in D_2O and then compared with pure EGCG and St under the same conditions (Fig. S5 and S6†). The representative ^{1}H NMR spectra showed that the proton signals belonging to EGCG and St shifted remarkably (Fig. 3b),[30,31] suggesting the successful complexation between them. To be specific, the chemical shifts of EGCG's H-2′,6′ and H-2″,6″ moved downfield from 6.43 and 6.86 to 6.60 and 7.01 ppm, respectively. In the meantime, the proton signals of H-a′ and H-a‴ in the St changed toward upfield from 5.45 and 4.95 to 5.34 and 4.87 ppm. These shifts may be due to the multiple hydrogen bonding between hydroxyl groups anchored on EGCG and St molecules, which enabled that the electrons flowed from the former to the latter. With the aim of acquiring information on their spatial correlations, rotating frame Overhauser effect spectroscopy (ROESY) 2D NMR spectra were detected (Fig. 3c). It was easy to observe the correlation between H-2′,6′ of EGCG and St's H-a′ and H-a‴ while H-2″,6″ in EGCG were just correlated with H-a′ in St. These correlations clearly declared that EGCG's benzene rings and glucose rings of St were close to each other, thus rationalizing the formation of hydrogen bonds in hydrogels. Besides, the strong correlation points in the 2D NMR spectrum unveiled a tight connection of two monomers, corresponding to the SEM observations. Eventually, we summed up all above results to propose a co-assembly mode. That is, the heating treatment promotes the dissolution and subsequent mixing of monomers, and then cooling serving as a critical factor triggers the self-assembly process from the view of thermodynamics. As illustrated in Fig. 3d, multiple and strong hydrogen bonding interactions between polyphenols and stevioside compounds provides the main driving forces for obtaining hydrogels and multi-path co-assembly leads to irregular network, which co-contributes to the formation of dense and disordered hydrogels. It is also noticeable that cooling was realized by standing at room temperature rather than thermal quenching, leaving required time for self-adaptation of monomers from the perspective of chemical kinetics. Therefore, the co-assembly should be a combination of thermodynamics and chemical kinetics.

3.3 Rheological properties of herbal hydrogels

To determine the mechanical property of EGCG–St hydrogel, various rheological tests were carried out. For the oscillatory shear rheology, when the strain exceeded 0.5%, the storage modulus (G')

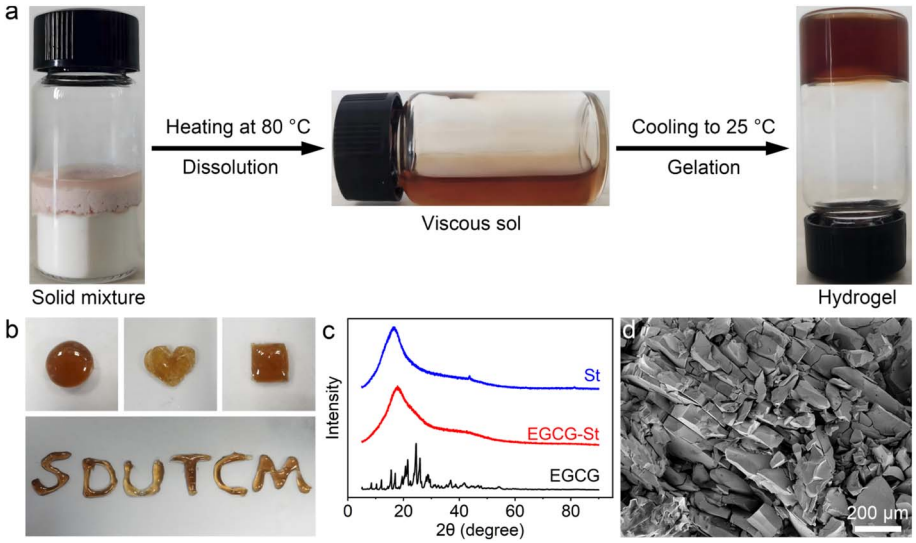

Fig. 1 (a) The preparation process of binary herbal hydrogels, and (b) corresponding hydrogel samples made in different molds, (c) XRD patterns of EGCG, St, and lyophilized EGCG–St hydrogel, and (d) typical SEM image of EGCG–St hydrogel.

became lower than the loss modulus (G''), indicating the transition from gel to sol state (Fig. 4a). Besides, the G' and G'' values were as high as 10^7 and 10^6 Pa, respectively. The results of dynamic frequency sweep showed that the values of G' were approximately 4 times larger than those of G'', and there was a weak dependency of EGCG–St hydrogel with frequency (Fig. 4b). According to the dynamic time sweep data, the constant G' and G'' values during the entire process revealed the good stability of hydrogel (Fig. 4c). In addition, temperature sweeps' results displayed that both the G' and G'' values obviously decreased as the temperature rising in the range of 25–100 °C (Fig. 4d). At nearly 100 °C, the G'' became larger than the G', corresponding to the occurrence of disassembly. Thus, it could be concluded that robust hydrogen bonding network not only rendered the valuable thermo-sensitivity property to the EGCG–St hydrogel, but also prevented it from collapsing below 100 °C. A macroscopic investigation of the thermal-responsive behaviour of hydrogels was conducted (Fig. 4e). The EGCG–St hydrogel at 90 °C became

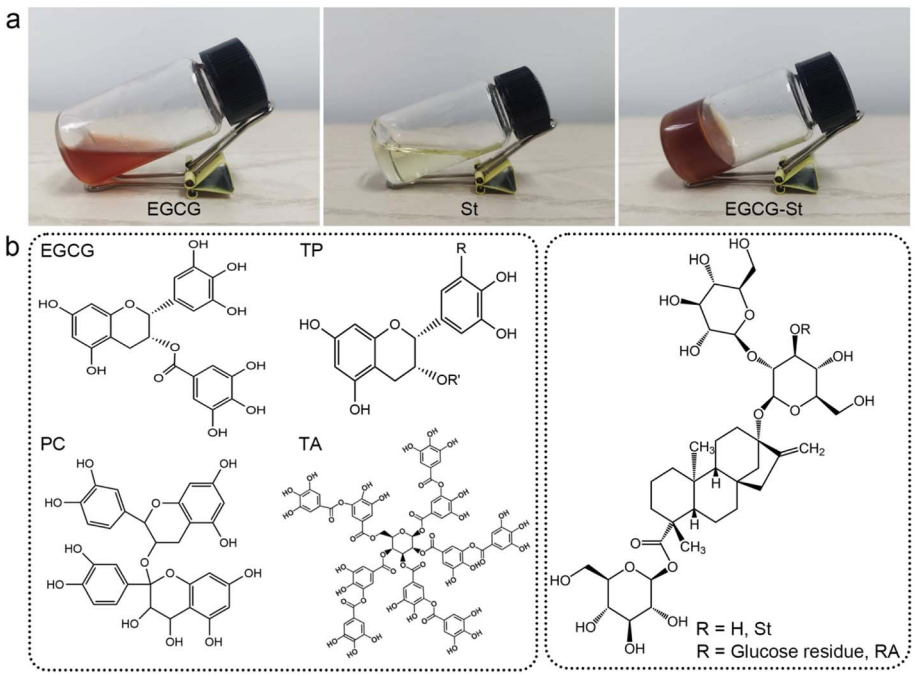

Fig. 2 (a) Photos showing the EGCG viscous sol (2.0 M), St aqueous solution (2.5 M), and corresponding EGCG–St hydrogel, and (b) the chemical structures of polyphenols and stevioside compounds used as hydrogel precursors.

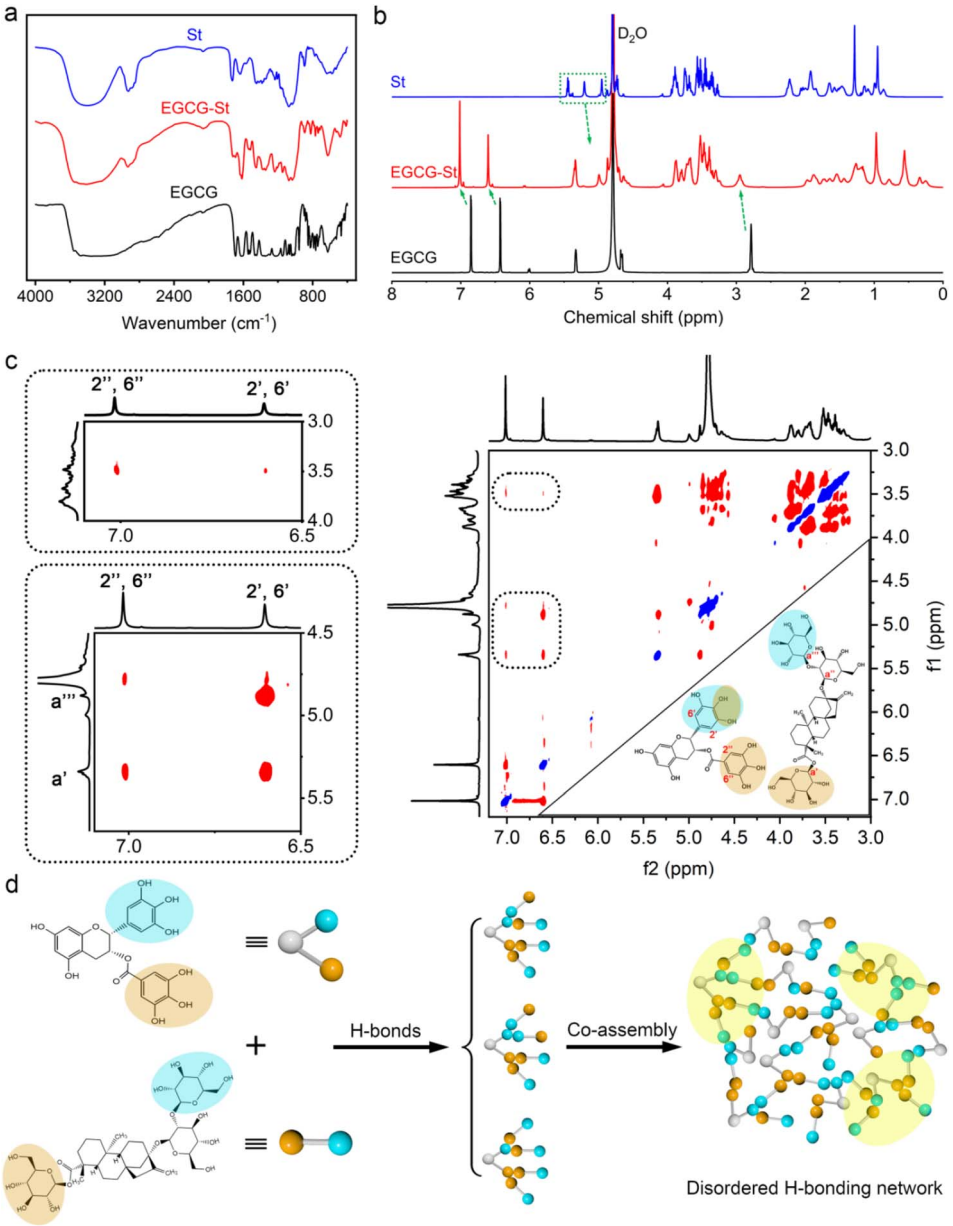

Fig. 3 (a) FT-IR spectra of EGCG, St, and EGCG–St hydrogel, (b) ^{1}H NMR spectra of EGCG, St, and EGCG–St mixture in D_2O, (c) 2D ROESY NMR spectrum (600 MHz) of EGCG–St mixture, and (d) the proposed co-assembly mode for the EGCG–St hydrogel.

viscous and began to flow slowly, attributed to its significantly decreased G' and G'' values. When the temperature was lowered to 25 °C, EGCG–St hydrogel could be restored and measured G' and G'' values were even slightly higher than the initial ones (Fig. S7†). The possible reason may lie in hydrogen bonding network in quasi-equilibrium state caused by the high solution viscosity and/or steric hindrance between EGCG and St molecules. Similar rheological behaviours were observed in other herbal hydrogels (Fig. S8 and S9–S11†). Moreover, Fig. 4f showed that the steady shear viscosity of EGCG–St hydrogel gradually decreased with increasing angular frequency, indicating that the hydrogel possessed shear thinning property and could be used for injection (Fig. S12†). Dynamic time sweep tests were also conducted after the hydrogel being injected through a syringe needle. It was found that the G' and G'' could return to original values after 2 hours (Fig. S13†). Considering that the injection could destroy the hydrogel due to its low critical strain value, the restoration of rheological properties proved the injectability and self-healing behaviour of the hydrogel.

3.4 Adhesive properties of herbal hydrogels

EGCG–St hydrogels were found to display strong and stable adhesion behaviors on different surfaces ranging from hydrophilic glass, ceramics, aluminium, and steel to hydrophobic polypropylene (PP), polyethylene (PE), rubber, and polytetrafluoroethylene (PTFE), meaning that they may serve as potential

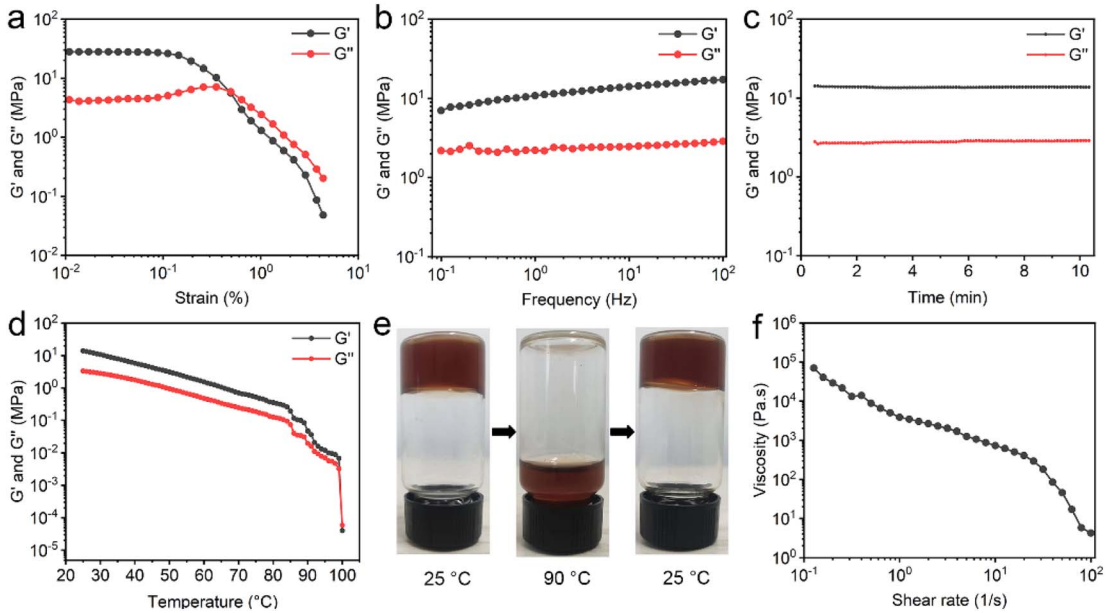

Fig. 4 (a) Strain-dependent oscillatory shear rheology with a fixed frequency of 10 rad s^{-1}, (b) dynamic frequency sweep measured at 0.1% strain, (c) dynamic time sweep at the strain of 0.1% and at the frequency of 10 rad s^{-1}, (d) temperature-dependent rheology of the EGCG–St hydrogel, (e) photos showing the thermo-responsiveness behaviour, and (f) the shear viscosity of EGCG–St hydrogel with shear rate ranging from 0.1 to 100 (1/s).

adhesive materials (Fig. 5a). Subsequently, quantitative tests were performed to measure the adhesion strengths of EGCG–St hydrogel on different substrates for comparing with other herbal hydrogels. Taking glass as an example, the hydrogel sample was deposited onto the surface of a glass slice and covered immediately by another glass slice, which was then utilized in single-lap shear tests. The adhesion strengths of EGCG–St hydrogel on steel, ceramics, and glass were 49.0, 39.2, and 53.0 kPa (Fig. 5b), respectively. Specially, ultra-strong adhesion effect between EGCG–St hydrogel adhesive and

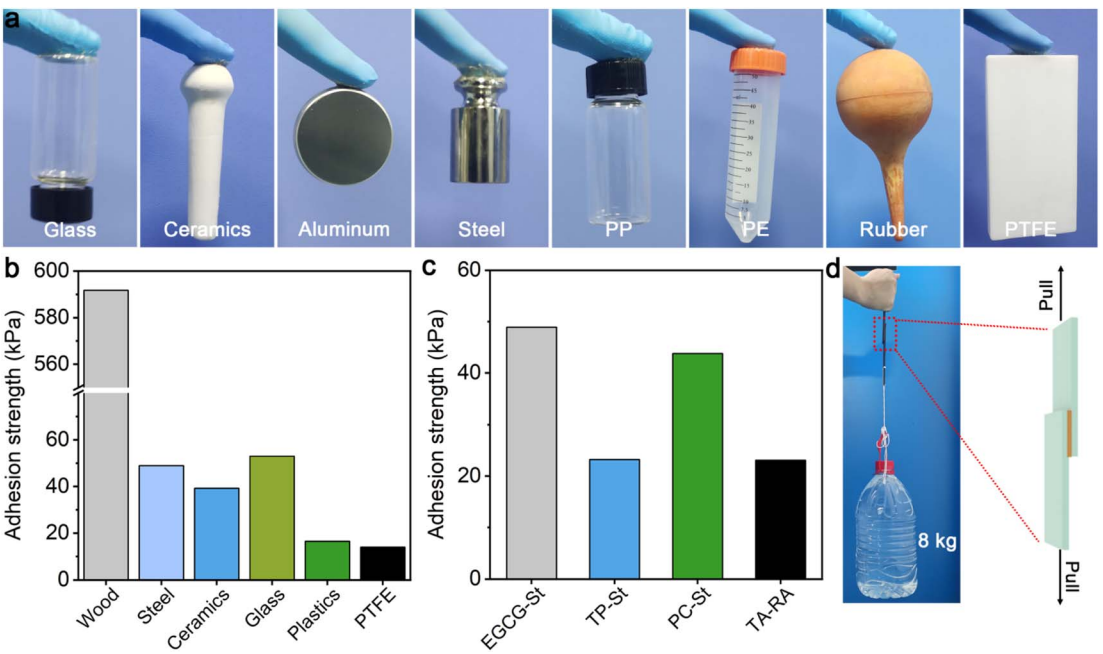

Fig. 5 (a) Images showing the macroscopic adhesion behaviours of EGCG–St hydrogel on various materials, (b) its adhesion strengths on wood, steel, ceramics, glass, plastics, and PTFE, (c) adhesion strengths of EGCG–St, TP–St, PC–St, and TA–RA hydrogels on steel, and (d) visual demonstration for the strong adhesion of EGCG–St hydrogel. (The adhesion area on wood substrate is 2 × 2 cm^2.)

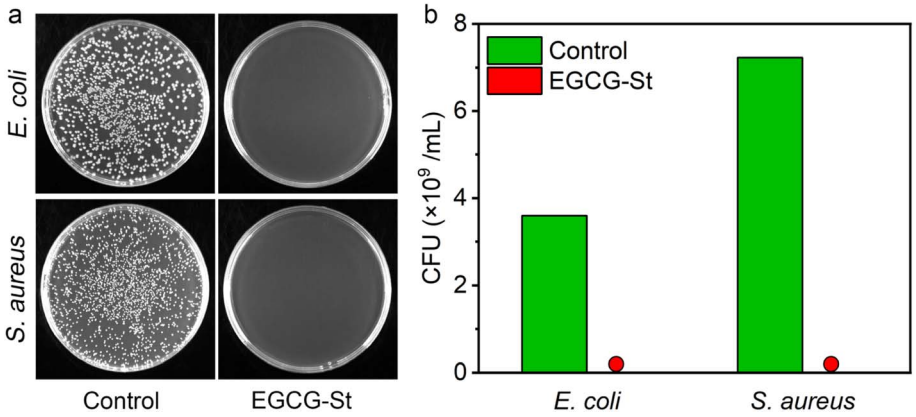

Fig. 6 (a) Representative photographs of agar plates of *E. coli* and *S. aureus* treated by EGCG–St hydrogel, and bacteria only were tested as controls, and (b) *in vitro* antibacterial activity of the EGCG–St hydrogel against *E. coli* and *S. aureus*.

wood surface was observed with the highest adhesion strength of 591.7 kPa. Unexpectedly, the EGCG–St adhesive materials exhibited satisfactory adhesion capabilities on hydrophobic surfaces. An adhesion strength of up to 16.5 kPa was obtained in the case of plastics. Though the EGCG–St adhesive materials showed the lowest adhesion strength on PTFE, the value of 13.9 kPa was still comparable with that of previously reported supramolecular or polymeric adhesives.[32–34] When comparing the adhesion effects of all herbal hydrogel materials, TP–St and TA–RA hydrogels possessed similar adhesion capacities on steel while EGCG–St and PC–St hydrogels had stronger adhesion strengths of 49.0 and 43.5 kPa, respectively. Hence, the adhesion strength of the herbal hydrogels could be modulated simply by adjusting the components and their concentrations. To further demonstrate the strong adhesion of EGCG–St hydrogel, a weight of up to 8 kg was attached to the adhered wood plates to exert shear forces, neither separation nor displacement of the adhesion area was observed (Fig. 5c).

3.5 Antibacterial assessment *in vitro*

Natural polyphenols such as EGCG and stevia extract St have been reported to have antibacterial effects.[35,36] Thus, we investigated the *in vitro* antibacterial activities of the prepared herbal hydrogels by flat colony counting method and *Escherichia coli* (*E. coli*) and *Staphylococcus aureus* (*S. aureus*) were used as model Gram-negative and Gram-positive bacteria, respectively. As shown in Fig. 6, it could be seen that there was almost no colony growth in the EGCG–St groups, indicating that the bacterial survival of both *E. coli* and *S. aureus* had been significantly inhibited after incubation with the EGCG–St hydrogel. Therefore, the EGCG–St hydrogel exhibited strong bacteriostatic capacity with almost 100% inhibitory effect on bacteria.

3.6 Fabrication of hydrogel coatings

Considering that the EGCG–St hydrogels possessed properties such as good processability, strong adhesion, and excellent bacteriostatic capacity, a three-step fabrication procedure was

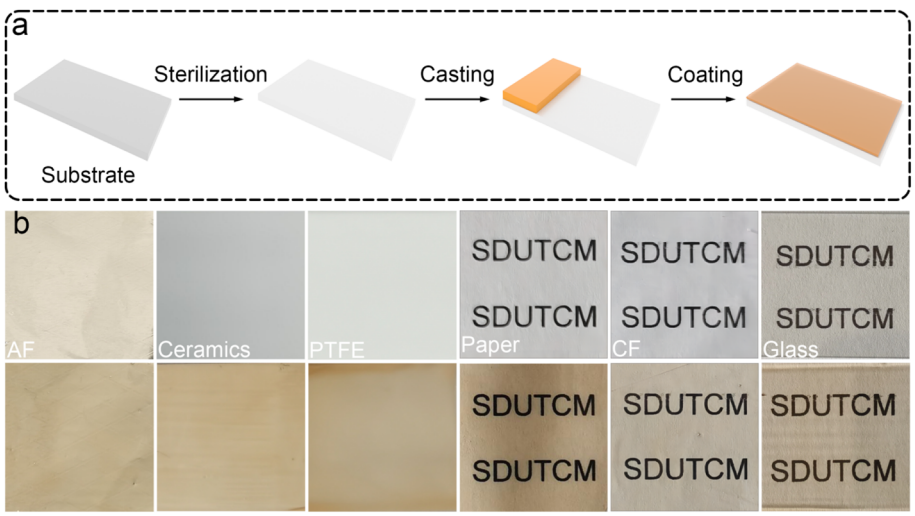

Fig. 7 (a) Schematic illustration of the fabrication process of the antibacterial coatings *via* coating method, and (b) photos of different substrates without (top) and with (bottom) hydrogel coatings.

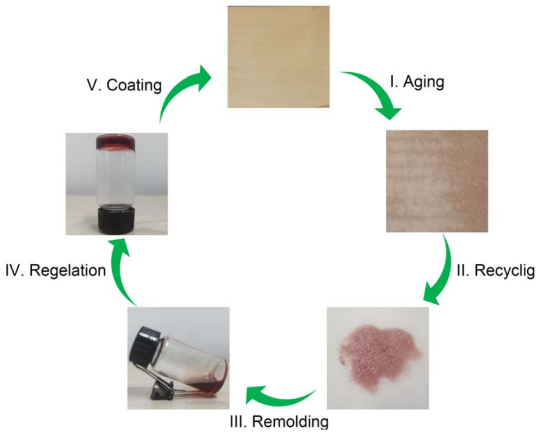

Fig. 8 Demonstration of the reusability of coatings based on herbal hydrogels.

developed to deposit hydrogel coating layers onto different substrates (Video S1†). As proposed in Fig. 7a, the substrate was subjected to UV sterilization to kill existing bacteria, followed by casting the EGCG–St hydrogels on the substrate surface. Finally, the substrate was fixed on a coating machine to achieve the coating layers. To explore the application scope of the EGCG–St hydrogel as coatings, diverse substrates including aluminium foil (AF), ceramics, PTFE, paper, cling film (CF), and glass were investigated (Fig. 7b). As a concept of proof, hydrogel coatings with thickness of about 0.3 mm were conveniently obtained for these substrates, and they were all colored in light orange. Generally, this kind of hydrogel coatings was quite smooth and uniform, and they were highly transparent to distinguish the words on/behind the substrates. Thus, the EGCG–St hydrogels had great potential in serving as natural antibacterial coatings.

Furthermore, these herbal hydrogel coatings were demonstrated to be recyclable and reusable in the aid of heating-induced regelation behaviour. The hydrogel coatings exposed to air for 10 days appeared with discernible crack owing to inevitable water loss.

The dried hydrogel fragments stripped from the substrate could turn into a viscous solution under high temperature (80 °C) after the addition of certain amount of water as medium. Similarly, the whole piece of hydrogel gradually reformed as the temperature decreased, and this amazing property enabled the hydrogel to be used again for coating preparation (Fig. 8). This cyclic process could be repeated for at least 5 times. Thus, the herbal hydrogel coatings possessed good reusability, which were superior to previously reported non-recyclable hydrogel coatings.[37–39] In fact, the functional failure of hydrogel coatings not only produces wastes to environment but also calls for more raw materials. Thus, from the view of sustainability, the present reusable herbal hydrogels might provide a promising solution to address this issue.

4. Conclusion

In summary, several binary herbal hydrogels were successfully prepared through a facile heating-cooling process with the multiple hydrogen bonding interactions serving as the main driving forces. Rheological tests revealed the high viscoelasticity, thermo-responsive ability, and shear-thinning property of hydrogels, endowing them with good processability. Besides, these herbal hydrogels were demonstrated to possess strong adhesion to both hydrophilic and hydrophobic surfaces. As a kind of natural hydrogels consisting of fully herbal small molecules, they also exhibit excellent antibacterial effects toward *E. coli* and *S. aureus*. Benefiting from these appealing features, the herbal hydrogels were deposited onto various substrates to fabricate thin coating layers, highlighting their great potentials as attractive natural antibacterial coatings. More importantly, this hydrogel coating could be reused *via* a temperature-induced remolding process. This study provides a simple and universal method to fabricate hydrogels based on binary herbal small molecules, which is of great significance for developing functional herbal hydrogel materials.

Conflicts of interest

The authors declare no conflict of interest.

Acknowledgements

We greatly acknowledge the financial support from the High Level Traditional Chinese Medicine Key Disciplines of the State Administration of Traditional Chinese Medicine, External Treatment of Traditional Chinese Medicine (zyyzdxk-2023116), general program of Shandong Natural Science Foundation (No. ZR2021MH373 and ZR2021LZY044), the fifth batch of National TCM clinical Excellent Talents Training Program (National TCM Education Word [2022] No. 1), Qilu Health and Health Leading Talents (Lu Wei Talent Word [2020] No. 3), and Jinan "GaoXiao 20 Tiao" Funding Project Contract (No. 2020GXRC005).

Notes and references

1 R. V. Ulijn, N. Bibi, V. Jayawarna, P. D. Thornton, S. J. Todd, R. J. Mart, A. M. Smith and J. E. Gough, *Mater. Today*, 2007, **10**, 40–48.
2 X. Cheng, L. Li, L. Yang, Q. Huang, Y. Li and Y. Cheng, *Adv. Funct. Mater.*, 2022, **32**, 2206201.
3 X. Xue, Y. Hu, S. Wang, X. Chen, Y. Jiang and J. Su, *Bioact. Mater.*, 2022, **12**, 327–339.
4 B. Hu, C. Owh, P. L. Chee, W. R. Leow, X. Liu, Y. L. Wu, P. Guo, X. J. Loh and X. Chen, *Chem. Soc. Rev.*, 2018, **47**, 6917–6929.
5 Y. Hou, L. Zou, Q. Li, M. Chen, H. Ruan, Z. Sun, X. Xu, J. Yang and G. Ma, *Mater. Today Bio*, 2022, **15**, 100327.
6 K. Zhi, J. Wang, H. Zhao and X. Yang, *Acta Pharm. Sin. B*, 2020, **10**, 913–927.
7 W. Y. He, X. C. Wang, W. Gong, H. B. Huang, Y. Y. Hou, R. Wang and J. N. Hu, *Colloids Surf., B*, 2023, **222**, 112975.
8 Y. Yang, D. Cai, Y. Shu, Z. Yuan, W. Pi, Y. Zhang, J. Lu, J. Jiao, X. Cheng, F. Li, P. Wang and H. Lei, *Mater. Des.*, 2023, **225**, 111435.

9 H. Huang, W. Gong, X. Wang, W. He, Y. Hou and J. Hu, *Adv. Healthcare Mater.*, 2022, **11**, 2102476.
10 J. Zheng, R. Fan, H. Wu, H. Yao, Y. Yan, J. Liu, L. Ran, Z. Sun, L. Yi, L. Dang, P. Gan, P. Zheng, T. Yang, Y. Zhang, T. Tang and Y. Wang, *Nat. Commun.*, 2019, **10**, 1604.
11 A. Saha, J. Adamcik, S. Bolisetty, S. Handschin and R. Mezzenga, *Angew. Chem., Int. Ed.*, 2015, **127**, 5498–5502.
12 W. Liu, Z. Li, Z. Wang, Z. Huang, C. Sun, S. Liu, Y. Jang and H. Yang, *ACS Appl. Mater. Interfaces*, 2023, **15**, 7767–7776.
13 Z. Pang, Y. Wei, N. Wang, J. Zhang, Y. Gao and S. Qian, *Int. J. Pharm.*, 2018, **548**, 625–635.
14 W. Li, *J. Mater. Sci.*, 2020, **55**, 6669–6677.
15 W. Liang, J. R. Guman-Sepulveda, S. He, A. Dogariu and J. Y. Fang, *J. Mater. Sci. Chem. Eng.*, 2015, **3**, 6–15.
16 B. G. Bag and S. S. Dash, *RSC Adv.*, 2016, **6**, 17290–17296.
17 J. Wu, J. Lu, J. Hu, Y. Gao, Q. Ma and Y. Ju, *RSC Adv.*, 2013, **3**, 24906–24909.
18 J. Zheng, X. Song, Z. Yang, C. Yin, W. Luo, C. Yin, Y. Ni, Y. Wang and Y. Zhang, *J. Controlled Release*, 2022, **350**, 898–921.
19 X. Guan, B. Zhang, Z. Wang, Q. Han, M. An, M. Ueda and Y. Ito, *J. Mater. Chem. B*, 2023, **11**, 4619–4660.
20 S. Wu, C. Cai, F. Li, Z. Tan and S. Dong, *CCS Chem.*, 2021, **3**, 1690–1700.
21 S. J. Bryant, M. N. Awad, A. Elbourne, A. J. Christofferson, A. V. Martin, N. Meftahi, C. J. Drummond, T. L. Greaves and G. Bryant, *J. Mater. Chem. B*, 2022, **10**, 4546–4560.
22 W. Zou, X. Lin and E. M. Terentjev, *Adv. Mater.*, 2021, **33**, 2101955.
23 S. R. Petersen, H. Prydderch, J. C. Worch, C. J. Stubbs, Z. Wang, J. Yu, M. C. Arno, A. V. Dobrynin, M. L. Becker and A. P. Dove, *Angew. Chem., Int. Ed.*, 2022, **61**, e202115904.
24 Z. Wang, Y. Zhang, Y. Yin, J. Liu, P. Li, Y. Zhao, D. Bai, H. Zhao, X. Han and Q. Chen, *Adv. Mater.*, 2022, **34**, 2270102.
25 F. Lin, Z. Wang, J. Chen, B. Lu, L. Tang, X. Chen, C. Lin, B. Huang, H. Zeng and Y. Chen, *J. Mater. Chem. B*, 2020, **8**, 4002–4015.
26 H. Liu, X. Hu, W. Li, M. Zhu, J. Tian, L. Li, B. Luo, C. Zhou and L. Lu, *Chem. Eng. J.*, 2023, **452**, 139368.
27 F. F. De Araújo, D. De Paulo Farias, I. A. Neri-Numa and G. M. Pastore, *Food Chem.*, 2021, **338**, 127535.
28 C. Gardana, P. Simonetti, E. Canzi, R. Zanchi and P. Pietta, *J. Agric. Food Chem.*, 2003, **51**, 6618–6622.
29 S. Gou, Q. Chen, Y. Liu, L. Zeng, H. Song, Z. Xu, Y. Kang, C. Li and B. Xiao, *ACS Sustainable Chem. Eng.*, 2018, **6**, 12658–12667.
30 J. Zhao, A. Blayney, X. Liu, L. Gandy, W. Jin, L. Yan, J. H. Ha, A. J. Canning, M. Connelly, C. Yang, X. Liu, Y. Xiao, M. S. Cosgrove, S. R. Solmaz, Y. Zhang, D. Ban, J. Chen, S. N. Loh and C. Wang, *Nat. Commun.*, 2021, **12**, 986.
31 N. Tangpaisarnkul, P. Tuchinda, P. Wilairat, A. Siripinyanond, J. Shiowattana and S. Nobsathian, *Food Chem.*, 2018, **255**, 75–80.
32 X. Liu, Q. Zhang, L. Duan and G. Gao, *ACS Appl. Mater. Interfaces*, 2019, **11**, 6644–6651.
33 J. Chen, J. Liu, T. Thundat and H. Zeng, *ACS Appl. Mater. Interfaces*, 2019, **11**, 18720–18729.
34 Y. Yan, S. Xu, H. Liu, X. Cui, J. Shao, P. Yao, J. Huang, X. Qiu and C. Huang, *Colloids Surf., A*, 2020, **593**, 124622.
35 P. Rani, X. Yu, H. Liu, K. Li, Y. He, H. Tian and R. Kumar, *Eur. Polym. J.*, 2021, **152**, 110494.
36 S. K. Yadav and P. Guleria, *Crit. Rev. Food Sci. Nutr.*, 2012, **52**, 988–998.
37 F. Zhang, C. Hu, L. Yang, K. Liu, Y. Ge, Y. Wei, J. Wang, R. Luo and Y. Wang, *J. Mater. Chem. B*, 2021, **9**, 2697–2708.
38 B. Fan, N. Cui, Z. Xu, K. Chen, P. Yin, K. Yue and W. Tang, *Biomacromolecules*, 2022, **23**, 972–982.
39 M. He, Q. Wang, W. Zhao, J. Li and C. Zhao, *Polym. Chem.*, 2017, **8**, 5344–5353.